The viscosity and ion conductivity of polydimethylsiloxane systems: 1. Chain length and ion size effects

J. E. Companik* and S. A. Bidstrup†
School of Chemical Engineering, Georgia Institute of Technology, Atlanta, GA 30332-0100, USA
(Received 22 June 1993; revised 30 March 1994)

The zero-shear-rate viscosity and ion conductivity of a homologous series of polydimethylsiloxane (PDMS) oils and six homologous series of PDMS salts of various univalent cations (sodium, potassium, tetramethylammonium, tetraethylammonium, tetrapropylammonium and tetrabutylammonium) were measured over the temperature range $-45°C < T < 80°C$. Free volume and Arrhenius type viscosity and ion conductivity models were successfully applied to these data. The effects of polymer chain length and ion size on the values of the best-fit model parameters were explored.

(Keywords: viscosity; ion conductivity; polydimethylsiloxane)

INTRODUCTION

In polymer systems, viscosity and ion conductivity are macroscopic properties that characterize chain segment mobility and ion mobility, respectively. Viscosity measures the response of polymer chain segments to an applied stress field. Ion conductivity measures the response of ions to an applied electric field. Although an inverse relationship between viscosity and ion conductivity has been observed[1-4], few studies have sought to obtain a basic understanding of (or quantitative relationship between) these important material properties.

A fundamental understanding of the ion conductivity of polymer systems and the development of relationships between ion conductivity, viscosity and changes in the polymer system have three important areas of application: the improved design and processing of polymer systems used in microelectronics encapsulation[5]; the design of superior polymer/salt complexes (polymer electrolytes) for use in electrochemical devices[6]; and the potential use of the measurement of ion conductivity as a means of polymer cure monitoring and control[4,7]. Yet, despite the need, theories and models describing ion motion in polymers most often do not relate to the microscopic picture and fail to predict how variables such as polymer chain length, polymer structure, ion size and ion concentration directly affect ion conductivity.

The goal of this investigation is to develop a fundamental understanding of chain segment and ion mobility in polymer systems. To this end, the effects of polymer chain length and ion size on the temperature-dependent zero-shear-rate viscosity and ion conductivity of one homologous series of polydimethylsiloxane (PDMS) oils and six homologous series of PDMS salts are determined. Moreover, Arrhenius and free volume type models with physically significant parameters are developed to relate changes in zero-shear-rate viscosity and ion conductivity to changes in the polymer systems. The PDMS systems were chosen for this study because they are commonly used as encapsulants in the microelectronics industry, have very low inherent ion impurity contents, and are characterizable over a wide temperature range ($-45°C < T < 80°C$ in this study).

THEORETICAL BACKGROUND

Viscosity of polymer systems

On a molecular level, viscous polymer flow is usually considered as the coordinated movement of small chain segments of whole polymer molecules[8]. These individual chain segment motions, in length on the order of 5–50 main chain atoms each in carbon chain systems, are assumed to be independent of each other. The net movement of whole polymer molecules, however, strongly depends on the *coordinated* movement of these individual segments. The generally observed phenomenon of increasing viscosity with increasing chain length is due to the fact that, as polymer chain length increases, a greater number of chain segments (units of flow) must coordinate to move.

Because polymer flow is dependent on the characteristics of both the whole chain structure and the local chain structure, models describing viscosity are usually developed as the product of two quantities: a structure factor and a segmental friction factor[9-11]. The structure factor is independent of temperature, reflects the length of the whole polymer chain, and assumes different expressions depending on whether or not complex chain interactions (i.e. chain entanglements) occur. The

*Current address: Motorola, Inc., Radio Products Group, 8000 W. Sunrise Blvd, Ft Lauderdale, FL 33322, USA
†To whom correspondence should be addressed

0032-3861/94/22/4823-11

segmental friction factor is determined by the temperature of the system and the local chain structure (the size of the unit of flow, the attraction forces between chain segments, and the fractional free volume of the system). Depending on the temperature range of interest, one of two different phenomena control this segmental friction factor. Therefore, a different theory of chain segment motion (and thus, polymer flow) is offered for each temperature range. Central to both theories is the fact that the free volume in a polymer system increases with temperature above the glass transition temperature (T_g), as described below.

Below T_g, the free volume in a polymer system is constant and below the minimum required for segmental mobility. T_g represents the onset of an increase in free volume (and thus, large scale segmental motion) with temperature. Therefore, close to T_g ($T < T_g + 100°C$), the limiting factor for chain segment motion is the availability of sufficient free volume for a chain segment to move. In this temperature region, free volume type models (e.g. the Doolittle, Williams–Landel–Ferry (WLF) and Berry–Fox expressions) are used to describe polymer flow[4,9–16]. The Berry–Fox model is of particular interest because of the physical significance of its parameters. The free volume viscosity model applied in this research is therefore developed according to the arguments of Berry and Fox.

The free volume viscosity model offered by Berry and Fox proposes that viscosity, η, is the quantity of a structure-sensitive factor, $F(Z)$, and a temperature-dependent segmental friction factor, $\zeta(T,f,z)$:

$$\eta = F(Z)\zeta(T,f,z) \tag{1}$$

The structure factor is independent of temperature, reflects the number of atoms in the backbone polymer chain (Z), and assumes different expressions depending on whether complex chain interactions (i.e. chain entanglements) occur. The segmental friction factor is dependent on the temperature of the system (T), the fractional free volume in the system (f), and the structure and size of the unit of flow ($z = 5$–50 main chain carbon atoms).

The structure-sensitive factor, $F(Z)$, is equal to the weight-average molecular weight (M_w) of the polymer raised to some power (a), as discussed previously[9]:

$$\eta = M_w^a \zeta(T,f,z) \tag{2}$$

where $a = 1.0$ for $M_w < M_c$ and $a = 3.4$ for $M_w \geq M_c$. M_c is the critical entanglement molecular weight.

The friction factor, $\zeta(T,f,z)$, characterizes the resistance to flow of a single polymer chain segment[16]. The magnitude of this friction factor depends on local intrachain and interchain forces between neighbouring chain segments and the availability of sufficient free volume for movement. Close to T_g ($T < T_g + 100°C$), the availability of free volume is the limiting factor in the mobility of a single chain segment. Therefore, the resistance to flow is directly related to the fractional free volume in the polymer system. As developed previously[9], the friction factor is of the form:

$$\zeta = \zeta_0 \exp\left[\frac{B}{f_g + (\alpha_1 - \alpha_0)(T - T_g)}\right] \tag{3}$$

where ζ_0 is the inherent friction factor, B is the fractional free volume required for chain segment motion, f_g is the ratio of void to occupied volume at T_g, α_1 is the volumetric thermal expansion coefficient of the liquid polymer, and α_0 is the volumetric thermal expansion coefficient of the occupied chain segment volume. The magnitude of the inherent friction factor (ζ_0) is believed to depend on the local intrachain and interchain forces between neighbouring chain segments[9]. The fractional free volume required for chain segment motion (B) is defined as the free volume required for a polymer chain segment to move, divided by the occupied volume of the chain segment. The entire segmental friction factor term, ζ, is therefore determined by temperature (T), polymer structure (ζ_0, f_g, $\alpha_1 - \alpha_0$ and T_g), and the relative size of the characteristic chain segment unit of flow (B).

The complete Berry–Fox free volume viscosity equation can therefore be expressed by substituting equation (3) into equation (2). This is simply the product of the structure-sensitive factor and the segmental friction factor:

$$\ln \eta = \ln M_w^a \zeta_0 + \left[\frac{B}{f_g + (\alpha_1 - \alpha_0)(T - T_g)}\right] \tag{4}$$

Far above T_g ($T > T_g + 100°C$), free volume availability is no longer the flow-limiting factor, as sufficient free volume for segmental motion exists in the system. In this temperature range, a polymer chain segment moves from its position to an unoccupied position by overcoming an apparent activation energy. Here, Arrhenius type models are used to model polymer flow[8–11,17–19]:

$$\eta = \eta_\infty \exp\left(\frac{E_\eta}{RT}\right) \tag{5}$$

where η_∞ is a pre-exponential factor which is a function of overall chain length, and E_η is the apparent energy of activation for chain segment motion.

Equation (5) fits the general definition of viscosity relationships for polymers developed in the beginning of this section. It is composed of a temperature-dependent component due to local chain structure (E_η/RT, the segmental friction factor) and a temperature-independent component due to whole chain structure (η_∞, the structure factor).

In this investigation, both the free volume (equation (4)) and Arrhenius (equation (5)) viscosity models, discussed above, will be applied to describe the temperature dependence of the viscosity of the homologous series of PDMS oils listed in *Table 1*. These models were chosen for this study because of the physical significance of their parameters. Therefore, changes in the polymer system should be reflected in changes in the best-fit model parameters.

Ion conductivity of polymer systems

Ion conductivity (σ) in a single charge carrier system (such as the PDMS systems examined in this study) is given by:

$$\sigma = nq\mu \tag{6}$$

where n is the mobile ion concentration, q is the magnitude of the ionic charges and μ is the mobility of the ions.

Table 1 Molecular weights and glass transition temperatures of the PDMS oils (PS438–PS443) and PDMS salts (SM438–SM443) used in this study

	Terminal group[a]	M_w	M_w/M_n	T_g (°C)
PS438	Vinyl	1200	1.14	−141
PS039.5	Trimethyl	2720	1.25	−128
PS040	Trimethyl	5190	1.20	−127
PS441	Vinyl	8700	1.28	−127
PS441.2	Vinyl	12800	1.33	−126
PS442	Vinyl	25900	1.42	−125
PS443	Vinyl	49300	1.59	−124
SM438	γ-M-n-propyl-carboxylate	1140	1.36	−117
SM039.5	γ-M-n-propyl-carboxylate	2650	1.29	−118
SM040	γ-M-n-propyl-carboxylate	5040	1.34	−122
SM441	γ-M-n-propyl-carboxylate	9560	1.43	−123
SM441.2	γ-M-n-propyl-carboxylate	12900	1.34	−123
SM442	γ-M-n-propyl-carboxylate	29900	1.45	−123

[a] M = TBA^+, TPA^+, TEA^+, TMA^+, K^+ or Na^+

In general, the concentration of mobile ions in a polymer system depends on the characteristics of both the polymer and the salt, as the driving force for ion solvation and transport in polymer/salt complexes involves interaction between Lewis base sites on the polymer (such as the lone pair electrons on oxygen atoms) and the cation[20]. In the case of cation solvation, groups of intrachain and interchain Lewis base sites present on the repeating unit of the polymer serve to attract or 'solvate' the cation. Larger ion salts have weaker cation–anion Coulombic attractions and are more easily solvated by a given polymer system than smaller ion salts. Also, because the solvation of one cation requires its coordination by as many as four Lewis base oxygen atoms[21], a given mobile chain segment is probably not involved in the solvation and transport of more than one cation at a time. Thus, the number of cations solvated by the polymer system (per unit volume) should increase with the number of mobile chain segments (per unit volume), regardless of the size of the segment. Therefore, a particular polymer system is able to solvate a finite amount of ions, dependent on the strength of its solvation sites, the size of the ions and the length of its unit of flow.

The mobility of an ion depends on its size and the mobility of the polymer chain segments. The mobility of an ion decreases with increasing ion size, which can be explained qualitatively by Stoke's law for the drift of a spherical object through a viscous medium[7]. Ion mobility is also directly related to the mobility of the polymer chain segments, as it is the repeated association of the cations with Lewis base sites on polymer chain segments, segmental motion with associated cations, and the dissociation of the cations that are responsible for cation transport in polymer systems[22].

Since ion conductivity is a function of both mobile ion concentration and ion mobility, models describing ion conductivity are usually developed as the product of two quantities: an ion concentration factor and an ion mobility factor. The ion concentration factor is slightly dependent on temperature and reflects the ability of the polymer to solvate a salt into mobile ions. Thus, the effective mobile ion concentration is a function of the structure of the polymer, the structure of the salt and the concentration of mobile chain segments. The ion mobility factor is strongly temperature dependent and is a function of the size of the ion and the mobility of the polymer chain segments (since polymer chain segment motion is necessary for ion motion).

Because of the strong theoretical and experimental relationships between ion conductivity and viscosity[1–4], arguments similar to those used to describe the temperature dependence of chain segment mobility are used to describe the temperature dependence of ion mobility. Close to T_g ($T < T_g + 100$°C), insufficient free volume for free movement leads to a decrease in chain segment mobility beyond simple Arrhenius behaviour. Thus, ion mobility should also decrease beyond simple Arrhenius behaviour, as the transport of ions strongly depends on the motion of polymer chain segments. A decrease in free volume may also lead directly to a decrease in ion mobility, if the ion itself is large enough to be limited in mobility by insufficient free volume for movement. Therefore, free volume type models are offered to describe ion motion in this temperature range. The types of models employed include semi-empirical WLF type expressions[20–32] and the Bidstrup–Simpson expression with its physically significant parameters[4].

Among the first researchers to model ion conductivity with semi-empirical WLF type expressions were Killis *et al.*[23], Berthier *et al.*[24] and Sheppard[25]. The modified WLF equation initially implemented by Sheppard expresses ion conductivity as:

$$\log\left[\frac{\sigma(T)}{\sigma(T_g)}\right] = \frac{C_1(T - T_g)}{C_2 + (T - T_g)} \tag{7}$$

where C_1 is a constant, and C_2 and $\log \sigma(T_g)$ were modelled assuming a linear dependency with the T_g:

$$C_2 = C_3 + C_4 T_g \tag{8}$$

and

$$\log \sigma(T_g) = C_5 + C_6 T_g \tag{9}$$

Although this modified WLF model can successfully predict the temperature dependence of ion conductivity in polymer systems, it requires the fitting of five empirical parameters. The empirical nature of the modified WLF model limits its utility as a fundamental research tool for understanding ion mobility in polymer systems. Therefore, it appears that a more physical modelling approach would be beneficial.

The free volume ion conductivity model developed by Simpson and Bidstrup[4] is unique in its theoretical approach and the physical significance of its parameters. This model employs free volume concepts similar to those used by Berry and Fox in the formulation of their viscosity model, and attempts to correlate ion mobility with polymer system structure through a dependency on the free volume in the system, the free volume required for an ion to move and the mobile ion concentration. Thus, formulation of this model begins with the same concepts employed in the development of the Berry–Fox viscosity model. However, because ion conductivity is directly related to the free volume in the system and inversely related to the free volume required for an ion to move, an ion mobility factor of the same form as the chain segment friction factor (i.e. the ratio of fractional free volume required for motion to the fractional free volume of the system) is inversely related to ion conductivity. Therefore, ion conductivity is the inverse

product of two quantities: an ion concentration factor, $F'(C_i)$, and the inverse of a temperature-dependent ion mobility factor, $\zeta'_0(T,f,B')$, which is of the same form as the segmental friction factor:

$$\sigma = F'(C_i)[\zeta'(T,f,B')]^{-1} \quad (10)$$

The ion concentration factor depends on the concentration of mobile ions (C_i) and is considered to be independent of temperature[22]. The ion mobility factor is determined by the measurement temperature (T), the fractional free volume of the system (f), and the fractional free volume required for an ion to move (B').

The effective ion concentration factor, $F'(C_i)$, is proposed to be a function of the mobile ion concentration (C_i), which depends on the solvation strength of the polymer, the strength of the salt and the concentration of mobile chain segments. Mobile ion concentration increases with an increase in the solvation strength of the polymer (which depends on polymer structure), an increase in the size of the ions of the solvated salt, and/or an increase in the concentration of mobile chain segments (which increases with a decrease in the size of the characteristic unit of flow).

The ion mobility factor, $\zeta'(T,f,B')$, is proposed to be a function of the measurement temperature (T), the fractional free volume of the system (f) and the fractional free volume (i.e. the ratio of void to occupied volume) required for an ion to move (B'). This factor characterizes the resistance an ion encounters when moving through the polymer system. Because of the free volume dependence, the ion mobility factor is proposed to be similar to the segmental friction factor in the free volume viscosity model (equation (3)):

$$\zeta' = \exp\left[\frac{B'}{f_g + (\alpha_1 - \alpha_0)(T - T_g)}\right] \quad (11)$$

where B', the fractional free volume required for ion motion, includes the free volume required for the movement of any polymer chain segments necessary for ion transport. Substituting equation (11) into equation (10), the free volume ion conductivity model becomes:

$$\ln \sigma = \ln F'(C_i) - \left[\frac{B'}{f_g + (\alpha_1 - \alpha_0)(T - T_g)}\right] \quad (12)$$

Far above T_g ($T > T_g + 100°C$), where a relatively large amount of free volume exists in the polymer system, the availability of free volume no longer limits chain segment or ion mobility. In this temperature range, an ion moves by overcoming an apparent activation energy. Therefore, Arrhenius type models are used to describe ion motion in this temperature region[23,24,33,34]:

$$\sigma = \sigma_\infty \exp\left(\frac{-E_\sigma}{RT}\right) \quad (13)$$

where σ_∞ is a pre-exponential factor and E_σ is the apparent energy of activation for ion motion. The pre-exponential term (σ_∞) depends on the concentration of mobile ions in the polymer system. The activation energy (E_σ) is the energy required to move an ion from its position to an unoccupied position, and should include the energy required to move any chain segments necessary for ion motion.

Equation (13) fits the general definition of ion conductivity relationships developed in the beginning of this section. It is composed of a temperature-dependent component determined by both chain segment mobility and ion size (E_σ/RT, the ion mobility factor) and a temperature-independent component determined by the effective mobile ion concentration (σ_∞, the effective ion concentration factor).

In this investigation, the free volume and Arrhenius ion conductivity models developed above will be applied to model the temperature dependence of the ion conductivity of the homologous series of PDMS salts listed in *Table 1*. These models were chosen for this study because of the physical significance of their parameters. Therefore, changes in the polymer system should be reflected in changes in the best-fit model parameters.

EXPERIMENTAL

PDMS oil systems

The α,ω-divinyl and α,ω-trimethyl PDMSs used in this study were purchased from Hüls America, Inc. These samples were purified before use by dissolving in methylene chloride, drying over anhydrous magnesium sulfate, vacuum filtering (pore size 4–5.5 μm), rotary evaporating at 35°C, and storing under full vacuum at 35–40°C for 16 h.

PDMS salt systems

The α,ω-bis(γ-M-n-propyl-carboxylate) PDMSs (where M is a univalent cation) used in this study were synthesized by neutralizing α,ω-bis(γ-n-propyl-carboxy) PDMSs with the appropriate hydroxide bases (M^+OH^-)[35]. The α,ω-bis(γ-n-propyl-carboxy) PDMSs were synthesized via a redistribution equilibration reaction between octamethylcyclotetrasiloxane and α,ω-bis(γ-n-propyl-carboxy) tetramethyldisiloxane (both from Hüls America, Inc.) in the presence of a sulfuric acid catalyst[36]. In this work, α,ω-bis(γ-M-n-propyl-carboxyl) PDMSs of the following cations were synthesized: sodium (Na^+), potassium (K^+), tetramethylammonium (TMA^+), tetraethylammonium (TEA^+), tetrapropylammonium (TPA^+) and tetrabutylammonium (TBA^+). These polymers were purified before use in the same manner as the α,ω-divinyl and α,ω-trimethyl PDMSs.

Nuclear magnetic resonance

The structure of each PDMS sample was verified by ^1H n.m.r. These spectra were obtained on a Varian XL-400 Nuclear Magnetic Resonance Spectrometer, using the undeuterated fraction of the methylene chloride solvent as an internal standard (chemical shift (δ) = 5.32 ppm).

Gel permeation chromatography

The weight-average molecular weight (M_w) and polydispersity (M_w/M_n) of each PDMS sample were determined by g.p.c. Analyses were performed at 35°C using a Waters Liquid Chromatograph System equipped with a Waters model 410 Differential Refractometer Detector and three Phenomenex Phenogel 5 g.p.c. columns (10^3 Å, 10^4 Å and 10^5 Å). Toluene was used as the carrier solvent. For the sake of comparison, the average molecular weights reported in *Table 1* are the

average molecular weights of the samples minus the relative contributions of the different end groups (vinyl, trimethyl or M-n-propyl-carboxylate).

Differential scanning calorimetry

The T_g of each PDMS sample was measured on a Seiko Instruments DSC220C Automatic Cooling Differential Scanning Calorimeter. A heating rate of 10°C min^{-1} was used. The T_g was taken as the midpoint of the change in heat capacity associated with T_g. The T_g of each PDMS sample is reported in *Table 1*.

Dilatometry

A Perkin–Elmer Series 7 Thermomechanical Analysis System, equipped with the extension probe and the dilatometer accessory, was used to measure the temperature-dependent volumetric thermal expansion coefficient of each PDMS sample over the range −50°C to 70°C.

Rheology

A Bohlin Instruments VOR Rheometer was used to measure the zero-shear viscosity of each PDMS sample over the temperature range −50°C to 80°C. The rheometer was equipped with the Fluids Head Option and the Low Temperature Measurement Option. Measurements were made using a parallel plate geometry consisting of a 25 mm upper plate and a 40 mm lower plate. The larger lower plate was used to ensure the correct edge profile for the low viscosity liquids studied. Thermal expansion of the test fixtures was accounted for in order to maintain a constant gap between the plates. At each temperature, the steady-shear viscosity of each sample was measured over a possible shear rate range of 3.37×10^{-3} to 2.65×10^{3} s^{-1}. The zero-shear viscosity was defined as the average steady-shear viscosity, when the steady-shear viscosity remained constant (Newtonian) over two decades of shear rates.

Dielectrometry

A Micromet Instruments Eumetric System III Microdielectrometer was used to determine the ion conductivity of each PDMS sample over the temperature range −45°C to 60°C. The microdielectrometer was equipped with the Low Conductivity Measurement Option and disposable 14 inch Low Conductivity Integrated Circuit Sensors. Temperature cycling was performed in a Fisher Scientific Isotemp Vacuum Oven (model 281A) for temperatures above room temperature. For sub-ambient temperature measurements, a thermoelectric heating/cooling module (Tellurex Corp.) with a dry-ice cold sink was used. At each temperature, the loss factor, $\varepsilon''(\omega)$, was measured over a frequency range of 0.1–10 000 Hz. The loss factor, $\varepsilon''(\omega)$, is a measure of the energy required for molecular motion in the presence of an electric field. It consists of energy losses due to the orientation of molecular dipoles, $\varepsilon_d''(\omega)$, and energy losses due to the conduction of ionic species, $\varepsilon_c''(\omega)$:

$$\varepsilon''(\omega) = \varepsilon_d''(\omega) + \varepsilon_c''(\omega) \tag{14}$$

Based on Debye's model of dipolar behaviour[37], $\varepsilon_d''(\omega)$ is a complex function of the relaxation time and the measurement frequency. The energy loss due to the conduction of ions, $\varepsilon_c''(\omega)$, is simply inversely proportional to frequency and equal to $\sigma/\omega\varepsilon_0$. Equation (14) can then be written:

$$\varepsilon''(\omega) = \varepsilon_d''(\omega) + \frac{\sigma}{\omega\varepsilon_0} \tag{15}$$

where ε_0 is the permittivity of free space equal to 8.85×10^{-14} F cm^{-1}. The dielectric loss factor is therefore dominated by energy losses due to ion conduction where $\varepsilon''(\omega)$ exhibits a linear dependency with $1/\omega$. The ion conductivity was thus defined as the average ion conductivity calculated from $\varepsilon''\omega\varepsilon_0$, when ε'' exhibited a linear dependency with $1/\omega$ over two decades of frequency.

Error analysis

The uncertainty in any data presented in this paper was calculated for a 90% confidence interval, assuming a Student's t distribution of the data.

RESULTS AND DISCUSSION

Viscosity of PDMS samples

The zero-shear-rate viscosity of each PDMS oil sample over the temperature range $-50°C < T < 80°C$ ($75°C < T - T_g < 205°C$ for PS039.5–PS443) is shown in *Figure 1*. The lower measurement temperature limit was fixed at approximately −50°C, as this is the temperature at which these silicone oils crystallize. The solid lines in *Figure 1* represent the best fits of Arrhenius (straight line) models (equation (5)) through the data in the temperature range $T - T_g > 100°C$. These lines are shown in order to demonstrate the slight curvature of the data at lower temperatures. Owing to crystallization, the data for PS438 ($T_g \approx -141°C$) did not extend into the temperature range $T - T_g < 100°C$, thus no curvature is evident. The best-fit Arrhenius model parameters (η_∞ and E_η) are reported in *Table 2*.

In the temperature range $T - T_g < 100°C$, free volume models (equation (4)) were used to fit the data (*Figure 2*). This model contains only two fitted parameters (f_g and B), as all of the other variables in this model were

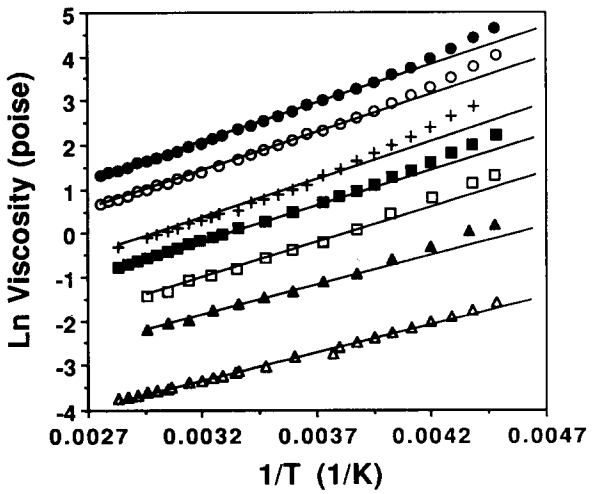

Figure 1 Temperature dependence of the steady-shear viscosity of PDMS oils. Solid lines represent Arrhenius model predictions (equation (5)) in the temperature range $T - T_g > 100°C$. ●, PS443; ○, PS442; +, PS441.2; ■, PS441; □, PS040; ▲, PS039.5; △, PS438

Table 2 Arrhenius (equation (5)) and free volume (equation (4)) viscosity model best-fit parameters for the PDMS oils

	Arrhenius model		Free volume model	
	ln η_∞ (poise)	E_η (kcal mol^{-1})	f_g	B
PS438	−7.45	2.43	–	–
PS039.5	−6.59	2.84	0.027	0.64
PS040	−6.45	3.38	0.035	0.84
PS441	−5.57	3.39	0.034	0.78
PS441.2	−5.09	3.37	0.028	0.77
PS442	−4.03	3.40	0.038	0.87
PS443	−3.40	3.42	0.040	0.89

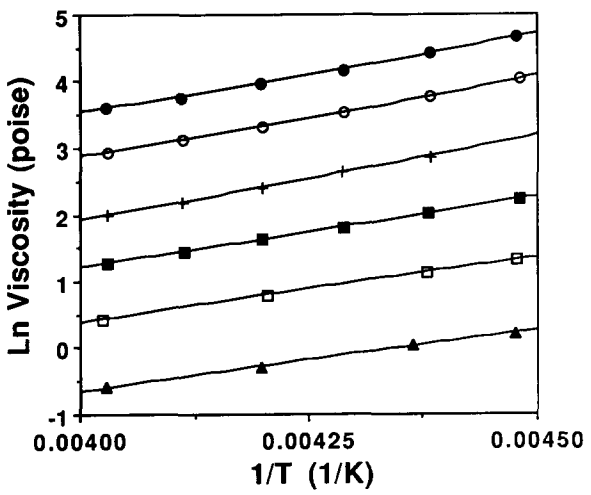

Figure 2 Temperature dependence of the steady-shear viscosity of PDMS oils. Solid lines represent free volume model predictions (equation (4)) in the temperature range $75°C < T - T_g < 100°C$. ●, PS443; ○, PS442; +, PS441.2; ■, PS441; □, PS040; ▲, PS039.5

determined independently. The M_w of each sample was determined by g.p.c. (*Table 1*). The critical entanglement molecular weight (M_c) of these PDMS oils was found[38] to be 63 000 through a series of viscosity experiments on a series of oils ranging from $M_w = 1200$ to 204 000; therefore, $a = 1$. An average ln ζ_0 was determined to be -12.15 ± 0.21 by extrapolating the high temperature viscosity data of each sample to $(T - T_g)^{-1} = 0$, since $\ln \eta = \ln M_w \zeta_0$ as $T - T_g$ approaches infinity (see equation (4))[39]. The volumetric thermal expansion coefficient of each liquid sample (α_1) was measured by dilatometry and determined to be independent of molecular weight for these samples, but dependent on temperature ($\alpha_1 = 1.39 \times 10^{-3} + 1.91 \times 10^{-6} T$(°C)). α_0 was assumed to equal zero[9]. The T_g of each sample was determined by d.s.c. (*Table 1*). The best-fit free volume model parameters (f_g and B) are reported in *Table 2*.

The best-fit parameters of both the Arrhenius and free volume models can be used to gain a better, quantitative understanding of polymer flow, as illustrated by the application of these models to the PDMS oil systems. Far above T_g ($100°C < T - T_g < 205°C$), where a relatively large amount of free volume exists in the PDMS system, a polymer chain segment moves from its position to an unoccupied position by overcoming an apparent activation energy. Thus, the activation energy for viscous flow (E_η) increases when the length of the characteristic unit of flow increases[8]. In the PDMS oils, E_η increases with M_w up to $M_w = 5190$ (PS040), where it levels off to 3.4 kcal mol^{-1}. This means that the unit of flow is the whole molecule for short molecules (PS438 and PS039.5), but only a segment of the whole molecule for long molecules (PS040–PS443). Dodgson *et al.*[19] found that E_η levelled off to 3.5 kcal mol^{-1} between $M_w = 3320$ and $M_w = 5020$ in a similar series of trimethyl-terminated PDMS. Therefore, it appears tht the length of the characteristic unit of flow in PDMS polymers is close to $M_w = 5190$. This corresponds to a weight-average number of repeat units (n_w) of 70, or 140 main chain atoms. It should be noted that this is a considerably longer unit of flow than that found in carbon backbone polymers (5–50 atoms)[8].

The component of the Arrhenius viscosity model dependent on the entire chain length of the polymer (η_∞) reflects the fact that polymer flow is the concerted movement of connected polymer chain segments for molecules longer than the characteristic unit of flow. Thus, η_∞ increases with M_w for PS040–PS443. However, no specific correlation between η_∞ and M_w for all polymer systems can be offered.

Close to T_g ($75°C < T - T_g < 100°C$), the limiting factor for chain segment motion is the availability of sufficient free volume for movement. The fractional free volume required for chain segment motion (B) increases when the size of the characteristic unit of flow increases[4]. In the PDMS oils, B increases from 0.64 for $M_w = 2720$ (PS039.5) up to an average value of 0.83 ± 0.05 for the higher M_w samples (PS040–PS443). This means that the unit of flow is the whole molecule for short molecules (PS438 and PS039.5), but just a segment of the polymer chain for long molecules (PS040–PS443), in agreement with the results of the Arrhenius modelling. The other fitted parameter in the free volume viscosity model is the fractional free volume in the PDMS oil system at T_g (f_g). The average value of f_g is 0.034 ± 0.004 for all samples, independent of M_w.

Berry and Fox found the ratio $f_g/B \approx 0.025$ for all carbon atom backbone polymers and $f_g/B \approx 0.080$ for PDMS systems[9]. In this study, $f_g/B = 0.041 \pm 0.007$ for PDMS systems. Berry and Fox reasoned that the deviation of the value of f_g/B for silicone polymers from the value of f_g/B for carbon polymers may reflect special structural features of the silicones (such as chain packing or intermolecular forces) not fully accounted for by the model. However, the value of f_g/B for silicones presented in this work is considerably closer to 0.025 than the value of Berry and Fox. Therefore, it appears that this difference between the silicone and carbon polymers may not be a limitation of the model, but a limitation of the small temperature range of data points used to model the case of silicone polymers. That is, these systems may not yet be in the temperature range at which free volume significantly limits chain segment motion at $75°C < T - T_g < 100°C$. Unfortunately, viscosity measurements on these systems were limited to a minimum temperature of $T - T_g \approx 75°C$, where these samples crystallize.

The zero-shear-rate viscosity of each PDMS salt sample was also measured over the temperature range $-45°C < T < 60°C$ ($75°C < T - T_g < 180°C$) (*Figure 3*). The ionic chain ends of these molecules form temperature-dependent ion pairs (and, possibly, ion aggregates), which effectively increase the molecular weights and viscosities of the samples[40–43]. Because these formations are temperature dependent, the effective molecular weight of each sample also changes with temperature, and there is

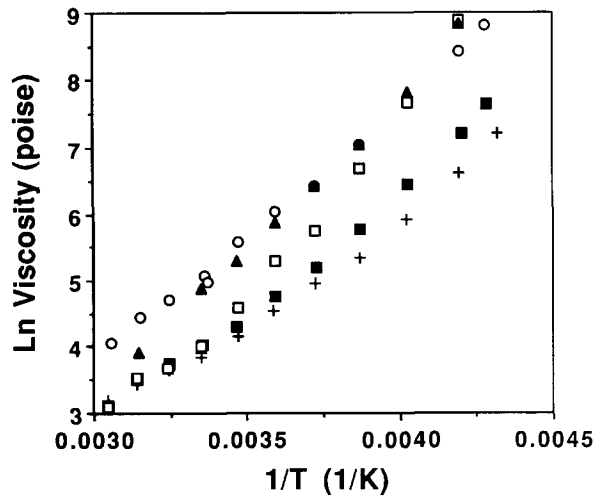

Figure 3 Temperature dependence of the steady-shear viscosity of PDMS salts in the temperature range $75°C < T - T_g < 180°C$. ○, SM442; +, SM441.2; ■, SM441; □, SM040; ▲, SM039.5

a greater increase in viscosity (compared with the PDMS oils) with decreasing temperature. Therefore, the Arrhenius and free volume viscosity models that were applied to the PDMS oil data could not be applied to the PDMS salt data, as these models assume a constant molecular weight. However, it can be assumed that the average f_g of the PDMS salts is the same as the average f_g of the PDMS oils ($f_g = 0.034$), since the T_gs of the salts are within 2–7°C of the highest T_g oil, and the liquid thermal expansion coefficients of the salts and oils are statistically identical ($\alpha_l = 1.39 \times 10^{-3} + 1.91 \times 10^{-6} T$ (°C)).

Also, the characteristic unit of flow of a PDMS salt is probably very similar to that of its corresponding nominal chain length PDMS oil. That is, a PDMS salt molecule most likely flows through the coordinated motion of chain segments the length of its nominal chain, because the repeating $Si(CH_3)$–O groups are more mobile than the dipole pairs. Therefore, the best-fit model parameters associated with the size of the characteristic unit of flow in the PDMS salts (E_η for the Arrhenius model, and B for the free volume model) are proposed to be the same for a PDMS salt as for a PDMS oil of the same nominal chain length.

Ion conductivity of PDMS samples

The PDMS oil samples (PS438–PS443) exhibited no measurable ion conductivity over the temperature range $-50°C < T < 60°C$ ($75°C < T - T_g < 185°C$). The lower limit of sensitivity of the conductivity measurement system used is 10^{-14} to 10^{-15} S cm^{-1} (ln $\sigma = -32$ to -34.5), varying between different disposable dielectric sensors.

Figure 4 shows the ion conductivity of each α,ω-bis(γ-sodium-n-propyl-carboxylate) PDMS salt sample over the temperature range $-45°C < T < 60°C$ ($75°C < T - T_g < 180°C$). The lower temperature limit was fixed at approximately −45°C, as this is the temperature at which these silicone salts crystallize. The solid lines in this figure represent the best fits of Arrhenius models (equation (13)) through the data over the entire temperature range. Arrhenius (straight line) models were fitted over the entire temperature range because none of the data for these Na^+ salts appear to curve, even at the lower temperatures ($75°C < T - T_g < 100°C$). Also, because the data for the longer chain length salts (SNa040–SNa442) were determined to be statistically identical, only one average line of best fit is shown for these salts in *Figure 4*. These two trends (Arrhenius behaviour throughout the temperature range $75°C < T - T_g < 180°C$ and similar temperature-dependent ion conductivity profiles for all of the high M_w samples) were also exhibited by the homologous series of K^+, TMA^+ and TEA^+ salts. The average best-fit Arrhenius model parameters (σ_∞ and E_σ) are reported in *Table 3*. The reported activation energies are average values for all chain length salts of a particular cation, as E_σ was statistically judged to be independent of chain length.

The temperature-dependent ion conductivities of the TBA^+ and TPA^+ salts do exhibit slight curvature in the lower temperature region ($75°C < T - T_g < 100°C$). *Figure 5* shows the ion conductivity of α,ω-bis(γ-tetrapropyl-ammonium-n-propyl-carboxylate) PDMS salt samples

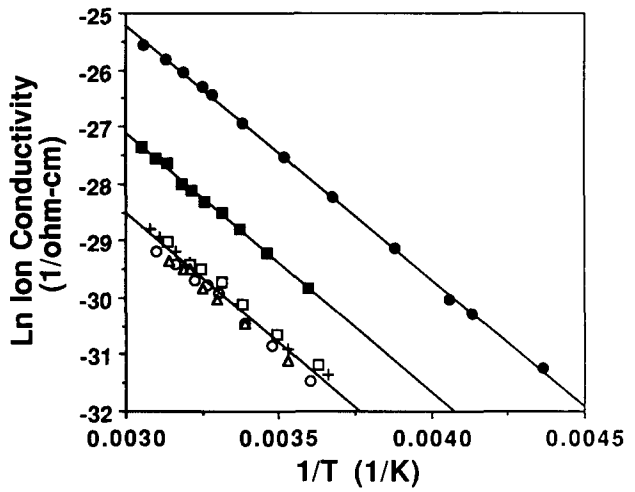

Figure 4 Temperature dependence of the ion conductivity of α,ω-bis(γ-sodium-n-propyl-carboxylate) PDMS salts. Solid lines represent Arrhenius model predictions (equation (13)) in the temperature range $75°C < T - T_g < 180°C$. ●, SNa438; ■, SNa039.5; +, SNa040; ○, SNa441; □, SNa441.2; △, SNa442

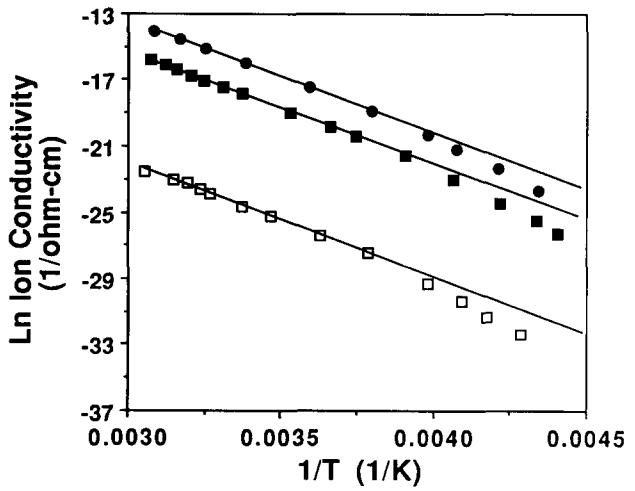

Figure 5 Temperature dependence of the ion conductivity of α,ω-bis(γ-tetrapropylammonium-n-propyl-carboxylate) PDMS salts. Solid lines represent Arrhenius model predictions (equation (13)) in the temperature range $100°C < T - T_g < 180°C$. ●, STPA438; ■, STPA039.5; □, STPA040. The data for STPA441, STPA441.2 and STPA442 were statistically identical to STPA040

Table 3 Arrhenius (equation (13)) and free volume (equation (12)) ion conductivity model best-fit parameters for the PDMS salts

	Arrhenius model		Free volume model	
	$\ln \sigma_\infty$ (S cm^{-1})	E_σ (kcal mol^{-1})	$\ln F'(C_i)$ (S cm^{-1})	B'
SNa438	-12.03 ± 0.53	9.1 ± 0.3	–	–
SNa039.5	-13.73	9.1	–	–
SNa040, 441, 441.2, 442	-15.12	9.1	–	–
SK438	-9.84	9.8	–	–
SK039.5	-11.01	9.8	–	–
SK040, 441, 441.2, 442	-13.31	9.8	–	–
STMA438	-6.97	11.6	–	–
STMA039.5	-8.96	11.6	–	–
STMA040, 441, 441.2, 442	-11.06	11.6	–	–
STEA438	1.75	12.7	–	–
STEA039.5	-0.52	12.7	–	–
STEA040, 441, 441.2, 442	-4.05	12.7	–	–
STPA438	6.72	13.6	-5.61 ± 0.53	2.5 ± 0.3
STPA039.5	5.40	13.6	-6.54	2.6
STPA040, 441, 441.2, 442	-2.10	13.6	-10.22	3.1
STBA438	–	–	2.16	3.0
STBA039.5	10.56	14.9	0.79	3.2
STBA040, 441, 441.2, 442	2.02	14.9	-0.48	4.8

over the temperature range $75°C < T - T_g < 180°C$. The solid lines in this figure represent the best fits of Arrhenius models (equation (13)) through the data in the temperature range $100°C < T - T_g < 180°C$. These lines are shown in order to demonstrate the slight curvature of the data at lower temperatures. Again, the data for the longer chain length salts were determined to be statistically identical. Thus, only one set of the high M_w salt data is shown in order to make the deviation from Arrhenius behaviour more apparent. The average best-fit Arrhenius model parameters (σ_∞ and E_σ) for the TBA^+ and TPA^+ salts in the temperature range $100°C < T - T_g < 180°C$ are reported in *Table 3*. The reported activation energies are average values for all chain length salts of a particular cation, as E_σ was statistically judged to be independent of chain length.

In the temperature range $75°C < T - T_g < 100°C$, a free volume model (equation (12)) was used to fit the ion conductivity data of the TBA^+ and TPA^+ salts. The free volume model fits for the TPA^+ salts are shown in *Figure 6*. This model contains only two fitted parameters ($F'(C_i)$ and B'), as all of the other variables in this model were determined independently. The steady-shear viscosity experiments determined $f_g = 0.034$ for these PDMS polymers. The volumetric thermal expansion coefficient (α_1) was measured by dilatometry and determined to be independent of molecular weight and identical to the value for the oils ($\alpha_1 = 1.39 \times 10^{-3} + 1.91 \times 10^{-6} T$ (°C)). α_0 was assumed to equal zero. The T_g of each sample was determined by d.s.c. (*Table 1*). The best-fit free volume model parameters ($F'(C_i)$ and B') for the TBA^+ and TPA^+ salts in the temperature range $75°C < T - T_g < 100°C$ are reported in *Table 3*.

The best-fit parameters of both the Arrhenius and free volume models can be used to gain a better, quantitative understanding of ion motion in polymers, as illustrated by the application of these models to the PDMS salt systems. Far above T_g, where a relatively large amount of free volume exists in the PDMS system, an ion moves from its position to an unoccupied position by overcoming an apparent activation energy (E_σ). E_σ includes both the energy required to move an ion from one Lewis base site to another and the energy required to move any chain segments necessary for ion motion (presumably, E_η). For these silicone systems, however, E_σ increases when ion size increases, independent of overall chain length, as shown in *Table 3*. Therefore, E_σ is apparently insensitive to the small differences in E_η exhibited by the silicone salts of different mobile chain segment lengths (assuming that the E_η of a salt is the same as the E_η of an oil of the same nominal chain length). Unfortunately, the E_η values of these PDMS salts cannot be determined directly, because of the chain end interactions discussed above.

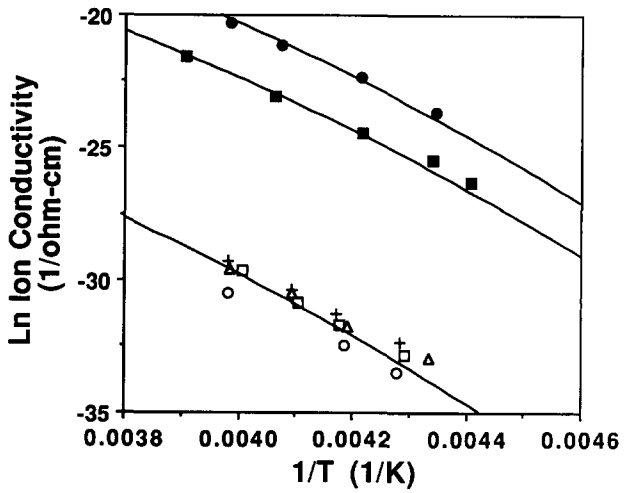

Figure 6 Temperature dependence of the ion conductivity of α,ω-bis(γ-tetrapropylammonium-n-propyl-carboxylate) PDMS salts. Solid lines represent free volume model predictions (equation (12)) in the temperature range $75°C < T - T_g < 100°C$. ●, STPA438; ■, STPA039.5; +, STPA040; ○, STPA441; □, STPA441.2; △, STPA442

On average, E_σ (*Table 3*) is three to four times the magnitude of E_η (*Table 2*). This indicates that ion conductivity is three to four times more temperature dependent than viscosity in these PDMS systems. Apparently, the process by which an ion transfers from one Lewis base site to another Lewis base site is much more thermally dependent than the process of a polymer chain segment moving from its position to an unoccupied position.

The component of the Arrhenius ion conductivity model dependent on the concentration of mobile ions in the system is the pre-exponential term (σ_∞), which reflects the solvation strength of the polymer, the length of the characteristic unit of flow and the size of the ions. The solvation strengths of all of the PDMS salts are assumed to be equal because these samples all have similar dielectric constants (≈ 2.7 at 25°C)[20,44]. Furthermore, the change in mobile ion concentration with temperature in similar polymer systems (poly(ethylene oxide) and poly(propylene oxide)) has been found to be negligible by other researchers[22]. Also, the fact that the pre-exponential term of the Arrhenius model does not change with temperature suggests that mobile ion concentration likewise does not change with temperature. Finally, the ionic chain end interactions discussed in the preceding section have been found to have no effect on mobile ion concentration[45]. The effects of chain length and ion size on σ_∞ are discussed, in turn, below.

As explained in the Theoretical Background section, a given polymer chain segment is most likely not involved in the solvation and transport of more than one cation at a time. Therefore, the number of cations solvated by a PDMS system (per unit volme) increases with the number of mobile chain segments (per unit volume). This trend is shown in *Figures 4* and *5*, and reflected in the values for σ_∞ in *Table 3*. For a particular cation salt, σ_∞ decreases as the size of the characteristic unit of flow (or mobile chain segment concentration) decreases. Ion conductivity shows no dependence on overall chain length because ion motion is dependent on the movement of individual chain segments only, not the concerted movement of connected chain segments (as is viscosity). Quantitatively, the concentration of mobile ions (as reflected in σ_∞) decreases an average of 6.5 ± 3.4 times between salts SM438 and SM039.5 and 6.4 ± 3.7 times between SM039.5 and SM040–SM442. The large uncertainty in the average values of σ_∞ makes further quantitative analysis hazardous, but from these data it appears that concentration of mobile ions in the PDMS systems is proportional to the size of the unit of flow raised to the -3.2 ± 0.6 power.

Salts of larger ions are more soluble than salts of smaller ions in a given polymer system. Thus, the concentration of mobile ions should increase with increasing ion size in these PDMS salt systems. This effect cannot be determined quantitatively by comparing values of σ_∞ for different cations of the same M_w, however, because salts of different cations have different activation energies (different slopes). Qualitatively, the difference in mobile ion concentration due to ion size is shown in *Figure 7*. In general, the temperature-dependent ion conductivity increases with the size of the cation; the data for the TMA^+ salt are the only exceptions. In the instances when the ion conductivity of a larger ion falls below that of a smaller ion, it is a reflection of the lower mobility of the larger cation (compared to the mobility of the smaller cation) dominating the observed ion conductivity.

In general, in polymer systems close to T_g, a decrease in system free volume may lead to a decrease in ion mobility either directly or through a decrease in the chain segment motion necessary for ion motion. In the PDMS salt systems, a decrease in chain segment mobility due to decreasing free volume near T_g ($75°C < T - T_g < 100°C$) apparently does not translate directly into a decrease in ion mobility, as no free volume curvature is observed for the smaller ion (Na^+, K^+, TMA^+ and TEA^+) salts in this temperature range. The curvature of the data for the TBA^+ and TPA^+ salts at low temperatures must therefore be a result of free volume constraints due to the size of the ions. Thus, the value of the fractional free volume required for ion motion (B') is larger for TBA^+ salts than for TPA^+ salts of the same mobile chain segment length.

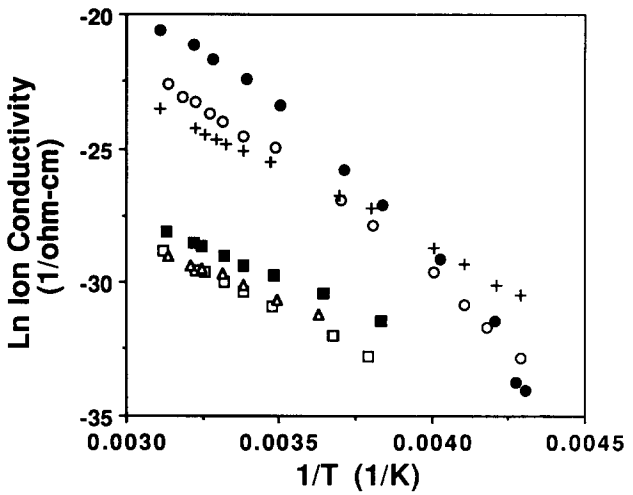

Figure 7 Temperature dependence of the ion conductivity of α,ω-bis(γ-M-n-propyl-carboxylate) PDMS salts of $M_w = 12900$. ●, STBA441.2; ○, STPA441.2; +, STEA441.2; □, STMA441.2; ■, SK441.2; △, SNa441.2

It is interesting to note that the fractional free volume required for ion motion is three to five times that required for chain segment motion, as determined by the B' and B parameters. In actuality, it is unlikely that three to five times more free volume is necessary for the movement of these ions, considering the size of an ion compared to the size of a 140-atom chain segment. However, the energy required to move an ion is three to five times the energy required to move a polymer chain segment as determined by the E_σ and E_η parameters. Perhaps the error lies in the definition of B', which should actually be considered as an effective volume required for ion motion, related to the energy required to move an ion. Therefore, further testing of this free volume model on large ion systems is required in order to determine whether B'/B continues to mirror E_σ/E_η.

The values of B' reported in *Table 3* also appear to increase with increasing mobile chain segment length. However, the difference in the B' values due to mobile chain length cannot be considered statistically significant because of their large uncertainties (± 0.4). Therefore, no conclusions about B' regarding chain length can be made.

The component of the free volume ion conductivity model dependent on the concentration of mobile ions in the system ($F'(C_i)$) is analogous to the σ_∞ term in the Arrhenius model. $F'(C_i)$ reflects the solvation strength of the polymer, the length of the characteristic unit of flow, and the size of the ions. Therefore, the concentration of mobile ions in the TBA^+ and TPA^+ salt systems (as reflected in $F'(C_i)$) decreases an average of 3.5 times between salts SM438 and SM039.5 and 4.2 times between SM039.5 and SM040–SM442. These are considerably smaller decreases than those estimated by the σ_∞ parameter, but they are within the large uncertainties associated with these decreases (6.5 ± 3.4 and 6.4 ± 3.7, respectively). Also, from the $F'(C_i)$ parameter data, it

appears that concentration of mobile ions in the PDMS systems is proportional to the size of the unit of flow raised to the -2.3 ± 0.8 power, which again is within the large uncertainty associated with the value determined from the σ_∞ parameters $(-3.2+0.6)$.

CONCLUSIONS

Depending on the temperature range, the zero-shear-rate viscosities of a homologous series of PDMS oils were successfully described by either Arrhenius ($100°C < T - T_g < 205°C$) or free volume ($75°C < T - T_g < 100°C$) models. The effects of polymer chain length on the best-fit parameters of these models were investigated.

From the Arrhenius model, the activation energy for viscous flow (E_η) increased with chain length until $M_w = 5190$, where E_η, and thus the length of the characteristic unit of flow, levelled off. Also, η_∞ was found to increase with chain length in PDMS longer than the characteristic unit of flow, but no relationship between η_∞ and M_w could be offered for all polymers.

From the free volume model, the fractional free volume required for chain segment motion (B) also increased with chain length and levelled off near $M_w = 5190$, confirming the length of the characteristic unit of flow determined by the Arrhenius modelling. The ratio f_g/B, determined by Berry and Fox to be 0.025 for carbon chain polymers and 0.080 for PDMS polymers, was found to be 0.041 ± 0.007 for these PDMS systems.

The temperature-dependent ion conductivities of six homologous series of PDMS salts of various univalent cations (Na^+, K^+, TMA^+, TEA^+, TPA^+, TBA^+) were also successfully described by either free volume or Arrhenius models. Arrhenius models were found to fit the data of the smaller ion salts (Na^+, K^+, TMA^+, TEA^+) over the entire temperature range studied ($75°C < T - T_g < 180°C$). The larger ion salts exhibited Arrhenius behaviour at higher temperatures ($100°C < T - T_g < 180°C$) and free volume behaviour at lower temperatures ($75°C < T - T_g < 100°C$). The effects of polymer chain length and ion size on the best-fit parameters of these models were investigated.

From the Arrhenius model, the activation energy for ion conduction (E_σ) increased with ion size and was independent of polymer chain length. Also, σ_∞ was found to increase with a decrease in the length of the characteristic unit of flow in a homologous series of a particular cation salt. Mobile ion concentration in these PDMS systems was determined to be proportional to the concentration of mobile chain segments raised to the 2.2 ± 0.6 power, using σ_∞ as a relative measure of mobile ion concentration. Mobile ion concentration also increased with increasing ion size, but σ_∞ could not be used to compare relative concentrations of different size cations (i.e. systems with different E_σ values).

From the free volume model, the fractional free volume required for ion motion (B') was found to increase with ion size in the two series of salts (TPA^+ and TBA^+) demonstrating free volume curvature. However, the large values of B' and the fact that B'/B' mirrors E_σ/E_η for these systems suggest that B' should actually be defined as an effective volume required for ion motion, related to the amount of energy required to move an ion. Also, $F'(C_i)$ was found to be a relative measure of mobile ion concentration, analogous to σ_∞ in the Arrhenius model. Using $F'(C_i)$ as a relative measure, mobile ion concentration in these PDMS systems was determined to be proportional to the concentration of mobile chain segments raised to the 1.6 power.

ACKNOWLEDGEMENTS

The authors gratefully acknowledge Dr Charles Liotta for his assistance in developing the PDMS salt synthesis route; Dr Leslie Gelbaum for performing the n.m.r. measurements; Ms Natascha Azzolin and Mr Frank Lin for performing the bulk of the d.s.c. measurements; Micromet Instruments for an equipment grant; and the Georgia Tech Manufacturing Research Center, the National Science Foundation (ESC-9058560), B. F. Goodrich and the Alcoa Foundation for their financial support.

REFERENCES

1 Kienle, R. H. and Race, H. H. *Trans. Electrochem. Soc.* 1934, **65**, 87
2 Lawless, G. W. *Polym. Eng. Sci.* 1980, **20**, 546
3 Kranbuehl, D. E. *J. Non-Crystalline Solids* 1991, **131–133**, 930
4 Simpson, J. O. and Bidstrup, S. A. *J. Polym. Sci.: Part B: Polym. Phys.* 1993, **31**, 609
5 Wong, C. P. *Adv. Polym. Sci.* 1988, **84**, 63
6 Ratner, M. A. and Shriver, D. F. *MRS Bull.* 1989, (**Sept.**), 39
7 Senturia, S. D. and Sheppard, N. F. *Adv. Polym. Sci.* 1986, **80**, 1
8 Billmeyer, F. W. 'Textbook of Polymer Science', 2nd edn, John Wiley and Sons, New York, 1984, p. 303
9 Berry, G. C. and Fox, T. H. *Adv. Polym. Sci.* 1968, **5**, 21
10 O'Conner, K. M. and Scholsky, K. M. *Polymer* 1989, **30**, 461
11 Lomellini, P. *Polymer* 1992, **33**, 4983
12 Doolittle, A. K. *J. Appl. Phys.* 1951, **22**, 1031
13 Doolittle, A. K. *J. Appl. Phys.* 1951, **22**, 1471
14 Doolittle, A. K. *J. Appl. Phys.* 1952, **23**, 236
15 Ferry, J. D. 'Viscoelastic Properties of Polymers', 3rd edn, John Wiley and Sons, New York, 1980, p. 287
16 Kumar, N. G. *J. Polym. Sci.: Macromol. Rev.* 1980, **15**, 255
17 Ewell, R. H. and Eyring, H. *J. Chem. Phys.* 1937, **5**, 726
18 Rosevare, W. E., Powell, R. E. and Eyring, H. *J. Appl. Phys.* 1941, **12**, 669
19 Dodgson, K., Bannister, D. J. and Semlyen, J. A. *Polymer* 1980, **21**, 663
20 Ratner, M. A. *Mater. Forum* 1991, **15**, 1
21 Papke, B. L., Ratner, M. A. and Shriver, D. F. *J. Electrochem. Soc.* 1982, **129**, 1434
22 Watanabe, M. and Ogata, N. *Br. Polym. J.* 1988, **20**, 181
23 Killis, A., LeNest, J., Cheradame, H. and Gandini, A. *Makromol. Chem.* 1982, **183**, 2835
24 Berthier, C., Gorecki, W., Minier, M., Armand, M. B., Chabagno, J. M. and Rigaud, P. *Solid State Ionics* 1983, **11**, 91
25 Sheppard, N. F. PhD Thesis, Massachusetts Institute of Technology, 1986, p. 239
26 Adamic, K. J., Greenbaum, S. G., Wintersgill, M. C. and Fontanella, J. J. *J. Appl. Phys.* 1986, **60**(4), 1342
27 Martin, G. C., Tungare, A. V. and Gotro, J. T. *Proc. Am. Chem. Soc. Div. Polym. Mater.: Sci. Eng.* 1988, **59**, 980
28 Kranbuehl, D., Delos, S., Hoff, M., Weller, L., Haverty, P. and Seely, J. *Am. Chem. Soc. Symp. Ser.* 1988, **367**, 100
29 Bidstrup, S. A., Sheppard, N. F. and Senturia, S. D. *Polym. Eng. Sci.* 1989, **29**(5), 325
30 Xu, K., Wan, G. and Tsuchida, E. *Polym. Adv. Technol.* 1992, **3**, 67
31 Kim, D., Ryoo, B., Maeng, K. and Hwang, T. *Polym. J.* 1992, **24**(6), 509
32 Lane, J. W., Khattak, R. K. and Dusi, M. R. *Polym. Eng. Sci.* 1989, **29**, 339
33 Rietman, E. A., Kaplan, M. L. and Cava, R. J. *Solid State Ionics* 1985, **17**, 67
34 Munshi, M. Z. A. and Owens, B. B. *Polym. J.* 1988, **20**(7), 577
35 Companik, J. E. *PhD Thesis*, Georgia Institute of Technology, 1993, p. 37
36 Kojima, K., Gore, C. R. and Marvel, C. S. *J. Polym. Sci., A1* 1966, **4**, 2325
37 Debye, P. 'Polar Molecules', The Chem. Cat. Co., New York, 1929, p. 106

38 Companik, J. E. *PhD Thesis*, Georgia Institute of Technology, 1993. p. 193
39 Companik, J. E. *PhD Thesis*, Georgia Institute of Technology, 1993. p. 198
40 Companik, J. E. *PhD Thesis*, Georgia Institute of Technology, 1993. p. 94
41 Otocka, E. P., Hellman, M. Y. and Blyler, L. L. *J. Appl. Phys.* 1969, **40**(11), 4221
42 Eisenberg, A. *Am. Chem. Soc. Div. Polym. Chem. Polym. Prepr.* 1988, **29**(2), 429
43 Roberts, C., Lindsell, W. E. and Soutar, I. *Br. Polym. J.* 1990, **23**, 55
44 Kobayashi, N., Sunaga, S. and Hirohashi, R. *Polymer* 1992, **33**, 3044
45 Companik, J. E. and Bidstrup, S. A. *Polymer* 1994, **35**, 4834